

Technical Notes

TECHNICAL NOTES are short manuscripts describing new developments or important results of a preliminary nature. These Notes cannot exceed 6 manuscript pages and 3 figures; a page of text may be substituted for a figure and vice versa. After informal review by the editors, they may be published within a few months of the date of receipt. Style requirements are the same as for regular contributions (see inside back cover).

J80-106 Design of Flat Plate Leading Edges to Avoid Flow Separation

M. R. Davis*

University of New South Wales,
Kensington, N.S.W., Australia

Nomenclature

a	= semimajor axis of elliptic nose
C_p	= surface pressure coefficient, $(p_s - p_0) / \frac{1}{2} \rho U_0^2$
l	= distance between center of nose arc and commencement of parallel surface = $\{2Rt(1 - r/t) + r^2 - t^2\}^{1/2}$
L	= length of parallel surface of plate
$M(\lambda)$	= polynomial function of λ
p_s	= surface pressure
p_0	= undisturbed flow pressure
R_{et}	= Reynolds number based on plate semithickness
R	= radius of second arc on leading-edge profile
r	= radius of nose arc on leading-edge profile
$2t$	= plate thickness
u	= local flow velocity parallel to surface
U_s	= flow velocity adjacent to surface
U_0	= undisturbed flow velocity
x	= streamwise coordinate
x_s	= coordinate along surface from stagnation point
δ	= boundary-layer thickness
λ	= boundary-layer parameter, $(\delta^2/\nu)(dU_s/dx_s)$
μ	= fluid viscosity
ν	= fluid kinematic viscosity
θ	= boundary-layer momentum thickness, $\int_0^\delta u/U_s(1 - u/U_s)dy$
ρ	= fluid density

I. Introduction

EXTREMELY sharp or extremely bluff leading edges on flat plate surfaces often lead to a local detachment of the laminar surface boundary layer. The flow may become turbulent before reattachment to the surface and is generally more susceptible to disturbances in the flow.¹ The use of an extremely sharp leading edge of half-wedge form is very sensitive to small flow misalignments and is often unacceptable where the flow may contain disturbances.^{2,3} Boundary-layer investigations have been carried out using a variety of curved leading edges⁴⁻⁶; the selection of the leading-edge contour is often made on an intuitive basis and subsequently modified if found necessary.³ The purpose of this Note is to determine for two simple leading-edge geometries which are easily specified, namely elliptical and double circular arc forms, what leading-edge shapes provide a fair margin as far as boundary-layer separation is concerned when the plate is at zero incidence.

Received Feb. 23, 1979; revision received July 23, 1979. Copyright © American Institute of Aeronautics and Astronautics, Inc., 1979. All rights reserved.

Index categories: Aerodynamics; Boundary Layers and Convective Heat Transfer—Laminar; Boundary-Layer Stability and Transition.

*Senior Lecturer, Dept. of Fluid Mechanics and Thermodynamics, School of Mechanical and Industrial Engineering.

II. Analysis and Results

The external potential flowfield was calculated using a numerical program⁷ which was designed to give accurate flow detail in the leading-edge region. It was assumed that the complete surface consisted of the shaped leading edge, a parallel section of length L ($L/t = 160$ being employed in the present calculations) and a wedge tapered trailing edge of length $10t$. The effects of the trailing-edge shaping on the leading-edge flow were quite negligible for these surfaces having a thickness/chord ratio of 0.53%. No boundary-layer displacement corrections were applied as it was estimated that these had a negligible effect for moderate thickness Reynolds numbers ($R_{et} = \rho U_0 t / \mu$) on the velocity distribution in the region of interest near the nose. The distribution of surface pressure coefficient in the nose region for the different shapes considered is shown in Fig. 1. The elliptical noses show a single minimum pressure region followed by a region of adverse pressure gradient as the flow velocity reduces to the external flow speed on the parallel section. The higher the axis ratio (a/t) of the elliptical nose, the smaller is the resultant minimum pressure coefficient, although the minimum then occurs further along the surface. The double arc noses show a minimum pressure, either on the larger radius of curvature

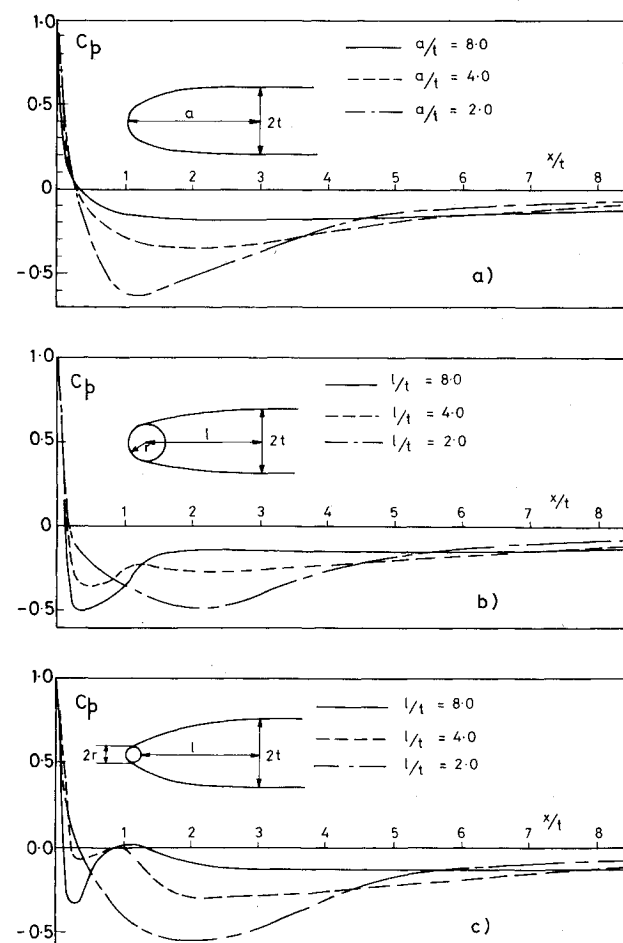


Fig. 1 Distribution of surface pressure coefficient: a) elliptical nose profiles, b) double arc nose profiles, $r/t = 0.5$, c) double arc nose profiles, $r/t = 0.25$.

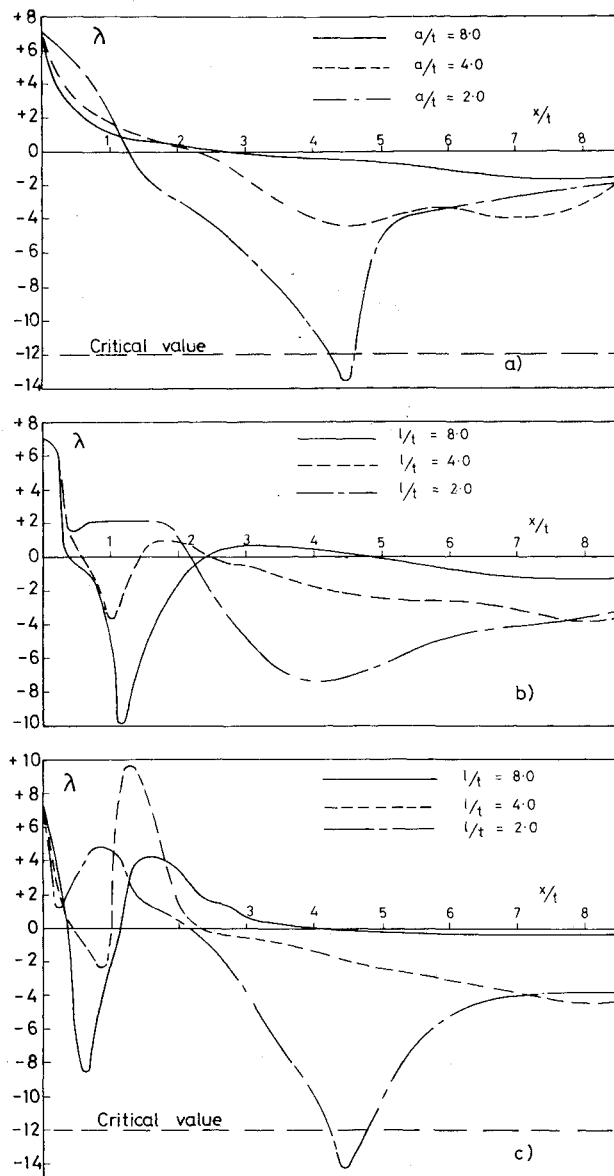


Fig. 2 Distribution of boundary-layer parameter: a) elliptical nose profiles, b) double arc nose profiles, $r/t=0.5$, c) double arc nose profiles, $r/t=0.25$.

second arc for small values of l/t , or on the smaller nose radius section for larger values of l/t . At intermediate values of l/t ($=8, 4$ in the present calculations) two minima can be observed and thus two regions of adverse pressure gradient, separated by a region of favorable pressure gradient, are formed.

Development of the boundary layer on the nose profiles will be determined on the basis of the momentum integral equation and the Pohlhausen family of velocity distributions.⁸ This family is characterized by the parameter $\lambda = (\delta^2/\nu)(dU_s/dx_s)$, where δ = boundary-layer thickness, ν = fluid kinematic viscosity, U_s = flow velocity tangential to surface, and x_s = distance following surface from front stagnation point. Boundary-layer separation occurs when $\lambda \leq -12$. Following Walz,⁹ the parameter λ may be determined by the equation:

$$M(\lambda) = \lambda \left\{ \frac{37}{315} - \frac{\lambda}{945} - \frac{\lambda^2}{9072} \right\}^2$$

$$= \frac{d(U_s/U_0)}{d(x_s/t)} \frac{0.40}{(U_s/U_0)^6} \int_0^{x_s/t} \left(\frac{U_s}{U_0} \right)^5 d\left(\frac{x_s}{t} \right)$$

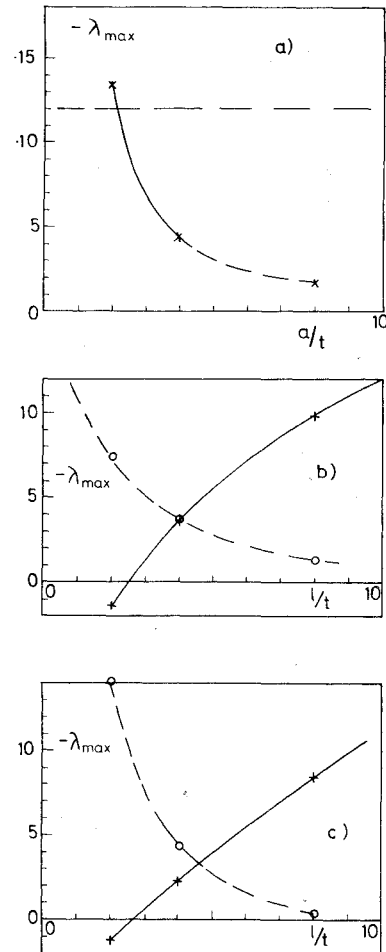


Fig. 3 Variation of minimum value of boundary-layer parameter with nose slenderness: a) elliptical nose profiles, b) double arc nose profiles, $r/t=0.5$, c) double arc nose profiles, $r/t=0.25$. (Solid line denotes minimum at forward position, dashed line denotes minimum at aft position).

It may be noted that λ is determined only by the form of the dimensionless velocity distribution U_s/U_0 as a function of x_s/t . The plate thickness Reynolds number does not enter the solution for $\lambda(x_s/t)$, as exactly compensating effects are introduced in the thickness and velocity derivative terms in the expression for λ . However, the thickness Reynolds number would provide an overall boundary to the range of applicability of the present calculations for laminar boundary layers. For $Re_t < 100$, approximately the assumption of a small layer thickness in relation to surface curvature and streamwise distance would no longer be a good assumption, while at higher Reynolds numbers, $Re_t > 5 \times 10^5$, turbulent transition might occur within the nose region analyzed. Also, the tendency to separate at a nonzero angle of attack (not considered here) is sensitive to thickness Reynolds number.

Putting $(U_s/U_0) = (1 - C_p)^{1/2}$ and evaluating distances along the curved surfaces (x_s/t) by a numerical procedure, values of $M(\lambda)$ were determined by integration along the surface. A simple iterative procedure was then used to determine λ from $M(\lambda)$; this converged rapidly as $M(\lambda) \approx 0.014 \lambda$ closely approximated the polynomial for $-12 < \lambda < 7$; the range extending from the front stagnation position ($\lambda = 7.05$) to a point of separation. The distributions of λ as a function of x/t which were thus obtained are shown in Fig. 2 for the elliptical and double arc noses. At intermediate values of the nose taper ($a/t=4, l/t=4$) it is seen that two minima are formed, although the effect is very weak in the case of the elliptical profile. For the double arc profiles

the first minimum occurs just after the change of curvature while the second occurs further downstream on the parallel section. The minima appear to be of comparable values in the particular cases shown.

Nose profiles having a more bluff aspect ($a/t=2$, $\ell/t=2$) show a very much stronger minimum λ at the further aft position on the surface, the particular cases considered indicating that separation would occur on the elliptical nose ($a/t=2$) and the smaller nose arc ($r/t=0.25$, $\ell/t=2$) profiles. Where the nose profile has a more slender aspect ($a/t=8$, $\ell/t=8$) the minimum at the more forward position is stronger.

The variation of the minimum value of λ with the nose slenderness parameters a/t and ℓ/t is shown in Fig. 3, separate curves denoting the minima at more forward or more aft positions. For the circular arc profiles it is seen that the tendency to separate may be minimized by selecting an intermediate value of ℓ/t ($\ell/t=4.0$ giving $-\lambda_{\max}=3.6$ for $r/t=0.5$ and $\ell/t=4.6$ giving $-\lambda_{\max}=3.2$ for $r/t=0.25$) such that the minimum λ at both positions is the same. It seems that the result is not strongly sensitive to the value of r/t in the range $0.25 < r/t < 0.5$ considered. If a greater margin to avoid separation is required, then an elliptical nose with $a/t > 5.0$ should be used when ($-\lambda_{\max}) < 3.0$ can be obtained. Experiments with a flat plate with a thickness Reynolds number between 1.5×10^4 and 5.0×10^4 and having an elliptical leading edge with $a/t=4.0$ were found to give no problems in the leading-edge area even when the plate was subjected to intense acoustical disturbances.²

III. Conclusions

The tendency for flow separation in the leading-edge region of a flat surface can be minimized using double arc contours with $r/t=0.25$ and $\ell/t=4.6$. Where a greater margin for boundary-layer separation near the nose is required, an elliptical leading edge with $a/t > 5.0$ should be used.

Acknowledgment

The support of the National Sciences Foundation and the Office of Naval Research while the author was at the Massachusetts Institute of Technology is gratefully acknowledged.

References

- ¹Chang, P. K., *Separation of Flow*, Pergamon Press, London, 1970.
- ²Shapiro, P. J., "The Influence of Sound Upon Laminar Boundary Layer Instability," *Acoustics and Vibration Laboratory*, Massachusetts Institute of Technology, Rept. No. 83458-83560-1, Sept. 1977.
- ³De Metz, F. C. and Casarella, M. J., "An Experimental Study of the Intermittent Properties of the Boundary Layer Pressure Field During Transition on a Flat Plate," Dept. of the Navy, NSRDC Rept. 4140, Nov. 1973.
- ⁴Kobashi, Y., Hayakawa, M., and Nakagawa, K., "Development of Disturbances in Unsteady Boundary Layers," *Symposium on Unsteady Aerodynamics*, Vol. 1, edited by R. B. Kinney, Arizona Board of Regents, Tucson, Ariz., 1975, pp. 131-153.
- ⁵Schubauer, G. B. and Klebanoff, P. S., "Contributing on the Mechanics of Boundary Layer Transition," National Advisory Committee for Aeronautics, Technical Rept. No. 1289, 1956.
- ⁶Knapp, C. F. and Roache, P. J., "A Combined Visual and Hot-Wire Anemometer Investigation of Boundary Layer Transition," *AIAA Journal*, Vol. 6, 1968, pp. 29-37.
- ⁷Milgram, J. H., "Slender Foil Computer Program AIR," Massachusetts Institute of Technology, Dept. of Ocean Engineering, private communication, 1975.
- ⁸Schlichting, H., *Boundary Layer Theory*, 6th ed., McGraw Hill, New York, 1968.
- ⁹Walz, A., "Ein neuer Ansatz für das Geschwindigkeitsprofil der laminaren Reihengsschicht," *Lilienthal-Bericht*, Vol. 141, 1941.

Effects of Swirl on the Subcritical Performance of Convergent Nozzles

20010
20016

P. W. Carpenter*
University of Exeter, Exeter, England

Introduction

SCHWARTZ^{1,2} has advocated the use of swirl as a possible method of noise reduction for turbojet and turbofan engines. His experimental data show considerable noise attenuation. On the other hand, the experimental results obtained by Lu et al.³ and Whitfield⁴ appear to be less promising. An important factor in assessing the suitability of swirl as a noise suppression device is the magnitude of the thrust loss incurred. Accordingly, a relatively simple method of estimating the effects of swirl on the mass flux and thrust of a subcritical convergent nozzle flow is presented below.

Some previous theoretical work has been reported on subcritical swirling flows in nozzles. For instance, Bussi⁵ compared Mach number distributions in a convergent-divergent nozzle obtained by numerical methods with the predictions of quasicylindrical theory. An approximate method is presented by Lu et al.,³ who apparently assume that the swirl angle remains constant across a nozzle section. It is shown herein that this method leads to substantially larger estimates of the thrust loss as compared to the present method. Experimental measurements of thrust and mass flux for subcritical swirling nozzle flows have been reported by Whitfield.⁴ These experiments were carried out at Rolls-Royce, Bristol, using single- and double-stage fixed-vane swirlers. Some of the data obtained are compared to theoretical predictions.

Analysis

It is assumed that the flow at the nozzle exit section is equivalent to a swirling flow in an infinitely long cylindrical duct. This is the so-called quasicylindrical assumption, which is analogous to the familiar one-dimensional theory for nonswirling nozzle flows. Furthermore, it is assumed that the swirl is produced by fixed vanes. This implies that for an inviscid non-heat-conducting gas the entropy and stagnation enthalpy are uniformly constant throughout the flow. Under these conditions Carpenter and Johannesen⁶ have shown that the Crocco vorticity theorem reduces to

$$\frac{v}{r} \frac{d(rv)}{dr} + w \frac{dw}{dr} = 0 \quad (1)$$

where v and w are, respectively, the tangential and axial velocity components at the nozzle exit and r the radial coordinate. Integration of Eq. (1) gives

$$w = \left(q_{\text{ex}}^2 - v_{\text{ex}}^2 + 2 \int_r^{R_{\text{ex}}} \frac{v}{r'} \frac{d(rv')}{dr'} dr' \right)^{1/2} \quad (2)$$

where $q^2 = v^2 + w^2$, subscript ex indicates conditions at the nozzle lip and R_{ex} is the radius of the nozzle exit section.

The pressure, p and density ρ at the nozzle exit are obtained from the isentropic flow relations, namely

$$\left(\frac{\rho}{\rho_0} \right)^{\gamma-1} = \left(\frac{p}{p_0} \right)^{(\gamma-1)/\gamma} = 1 - \frac{\gamma-1}{\gamma+1} (W^2 + V^2) \quad (3)$$

Received May 8, 1979; revision received Nov. 7, 1979. Copyright © American Institute of Aeronautics and Astronautics, Inc., 1979. All rights reserved.

Index categories: Nozzle and Channel Flow; Subsonic Flow.

*Lecturer, Dept. of Engineering Science. Member AIAA.